Investigations of surface morphology and chemical composition of Ag/ZnS/glassceramic thin-film structure

D. Kurbatov[1], A. Opanasyuk[1], V. Denisenko[2], A. Kramchenkov[2], M. Zaharets[2]
[1]*Sumy State University, Department of General and Experimental Physics,*
2, Rimsky-Korsakov str., 40007 Sumy, Ukraine, e-mail: kurd@ukr.net
[2]*Applied Physics Instiute, 58, Petropavlovskaya str., 40030 Sumy, Ukraine*

Abstract. The surface morphology and chemical composition of Ag/ZnS/glassceramic thin-film system obtained by close-spaced vacuum sublimation technique under different grow conditions were investigated. Examination of surface profile and morphology was performed by scanning electron and optical microscopy. Chemical composition was studied by Rutherford back scattering method. Results of morphology studies enabled to determine dependence of the growth mechanism, roughness R_a, grain size D of ZnS layers on the growth conditions. The researches of chemical composition allowed to determine the concentration of compound elements and impurities, deviation from stoichiometry and thickness distribution of chemical elements.

1. Introduction

Thin-film solar cells with $Cu(In_{1-x}Ga_x)Se_2$ (CIGS) and $CuInS_2$ (CIS) absorbers have achieved high efficiencies in recent years. Cadmium sulfide (CdS) buffer layers prepared by chemical bath deposition (CBD) are commonly used in CIGS or CIS-based cells. Even though cells with the ZnO/CBD-CdS/CIGS structure have high efficiencies ($\eta = 19.6$ %), manufacturing companies have sought alternatives to the CBD-CdS buffer layer, which could eliminate the use of Cd ("Cd-free") and improve the collection of carriers generated by shortwave light [1]. One promising alternative material is ZnS. Its bandgap energy (E_g) of 3.68 eV makes it transparent to practically all wavelengths of the solar spectrum. In contrast, CdS with its bandgap of 2.4 eV is highly absorbing for wavelengths below 520 nm.

There has been a considerable progress in using CBD-ZnS in CIGS-based thin-film solar cells. The best efficiency of ZnO/CBD-ZnS/CIGS solar cells increased to 18.6 % [2] in recent years. As one of the possibilities of efficiency improving, there is chemically pure growth of ZnS buffer layer with a high coefficient of optical transmission. But it is possible only by replacing the deposition method to receive condensates, since according the literature CBD-ZnS contains significant amounts of oxygen in the form of ZnO and/or $Zn(OH)_2$ in its composition.

This work is devoted to chemical composition and morphology studies of ZnS thin films obtained by close-spaced vacuum sublimation technique (CSVS) under different grow conditions. It is considered that the close-spaced vacuum evaporation method (CSVE) may become successful alternative to CBD method for producing the ZnS-based window layer of solar cells with improved characteristics [3].

Under the deposition of ZnS films exercisable as basic layers of solar cells, the optimization of film characteristics is very important. These condensates on cheap glass substrates must have monophase columned structure with low level of non-controlled impurities and composition close to stoichiometric. It stipulated the aim of this paper.

2. Experimental details

Thin ZnS films were obtained by CSVE method [4]. The refined glassceramic plates were used as substrates. The evaporation of two-phase stoichiometric ZnS powder was carried out. The temperature T_e of the evaporator was 1373 K. The temperature T_s of substrate was varied within the range 373 to 973 K. The time t of layer condensation was 300 s. The thickness of films L was varied within the range 0.2 to 7 μm. Geometry of our samples was determined by the mask in-use. Usually they had a shape of a circle with a diameter 10 mm. The

thin Ag layer was applied on the ZnS film to support gathering the charge from the film surface during measurements using charge particles. Under these conditions, the temperature of the ZnS surface was 373 K.

The morphology of ZnS films surface was investigated by scanning electron (SEM 103-01) and optical microscopy. The average grain size D inside the layers was determined by the Jeffries method by using the formula $D = k\sqrt{S/M^{-2}n}$, where k is the coefficient of grain shape, S – the area of the section in a micrograph; M – magnification; n – the number of grains in a chosen plot. The calculation of surface roughness was performed according to the standard ISO/R 468 [5], while the average arithmetic deviation R_a of profile was defined by formula $R_a = \frac{1}{n}\sum_{i=1}^{n} y_i$, where y_i – profile deviation of film surface from the mean line, n – the number of profile peaks.
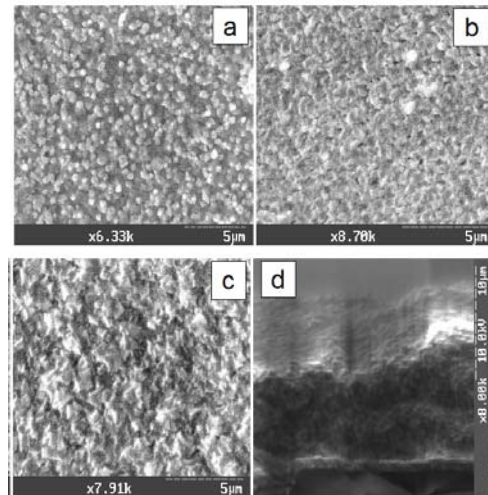
To determine elemental composition of Ag/ZnS/glassceramic, the Rutherford backscattering method (RBS) of protons was used [6]. As the source of charged particles, the electrostatic accelerator on 1 MeV (Institute of Applied Physics, NAS of Ukraine) was utilized. The primary beam of protons bombarded the target normally, scattering angle was 135°. As the detecting system, the magnetic spectrometer and Si-detector of charged particles were used. This magnetic spectrometer allowed to enhance the energy resolution to 3.2 keV.

The RBS spectra processing was performed by the SIMNRA program. Determination of the impurity concentration and component depth profiles for this compound was fulfilled by means of standard technique [7].
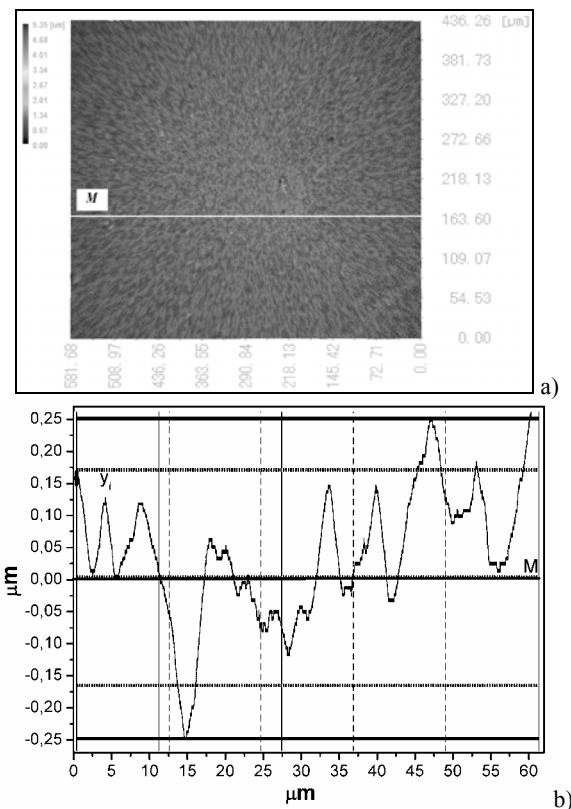
3. Results and discussion

As a result of pursued researches of ZnS films in Ag/ZnS/glassceramic structure surface morphology, it was determined that these films are polycrystalline, homogeneous along the samples area and they have good adhesion to substrate for deposition temperatures $T_s > 300$ K (Fig. 1). At low temperatures the film substrates were fine-crystalline ($D < 0.1$ µm). Through intensive secondary nucleation, at the same time growth of crystallite dimensions with increasing of film thicknesses almost didn't take place.

With increasing T_s, the growth mechanism varied, and the films began to grow according to the column-like mechanism. While increasing T_s from 323 to 993 K, the average size D of crystallite in the film plane grew from 0.1 µm to 1-2 µm at $L \sim 3$ µm. D increase occurred also while L increasing. Under conditions close to thermodynamic equilibrium, the films were practically monoblock along the layer thickness.

Fig. 1. Microstructure of ZnS films: surface morphology of the films grown under various substrate temperatures: $T_s =$ 393 K (a); 573 (b); 993 (c); and their cross-section (d).

The investigation of optical characteristics of condensates [8] demonstrated that for the wavelength λ greater than 350-360 nm the significant enhancement of the transmission coefficient occurred and for λ greater than 450-500 nm all the films had a very high transmission coefficient that ran up to 85-95 %. This argues about availability to use vacuum ZnS condensates as a high-energy gap window of thin-film solar cells.

Fig. 2. Typical optical migrograph of the ZnS film (a) grown under $T_s = 863$ K and profile of the surface part (b).

The surface morphology investigation of ZnS films, fulfilled in this work, revealed that the rise of the condensation temperature is going with increase in height of layers relief and therefore its surface roughness. The typical micrographs of condensate surfaces and surface profilograms are presented in Fig. 2. For quantitative estimation of films roughness by using the profilograms, the calculation of average arithmetic deviations of profiles R_a from the average line was performed.

Determination of the parameter R_a shows that under rising temperature from $T_s = 423$ K to 863 K the surface roughness is increased from $R_a \approx 0.062$ μm to 0.147 μm at $L \sim 3$ μm. The dependence of the profile average arithmetic deviation for ZnS films versus T_s is shown in Fig. 3.

In Fig. 3, two regions of temperature with different R_a – dependences on the temperature T_s might be indicated. Their presence may be explained by changing the mechanism of ZnS films growth under $T_s > 650$-700 K. The sharper arising of average arithmetic deviation R_a of films surface profile occurs in the range of deposition temperature, where the column mechanism of film growth is realized.

It is known that solar cells with heterojunctions are fabricated in two configurations: back- and frontal-barriered. The maximal efficiency is inherent to back-barriered structures, where the electrically conductive transparent layer of ZnO (SnO_2) or its analogue is initially deposited on the glass substrates, then ZnS buffer layer follows and finally the basic light-absorbing layer (CIGS or CdTe) with current-collecting contact completes the block. Using ZnS films with the columned structure and comprehensive surface relief must promote improving the efficiency of corresponding solar cells through reduction of reflectivity factor from basic layer surface and series connected resistance relating to presence of grain boundary.

The typical proton-scattering spectra obtained from films deposited under various physical and technological conditions are represented in Fig. 4a. In Fig. 4b, the simulated with program package SIMNRA [9] RBS spectra accompanied with the measured ones are represented. The reconstruction degree of experimental spectra is very high. As shown in Fig. 4, the elements that belong to substrate and current-collecting contact contribute to RBS spectra besides ZnS compound.
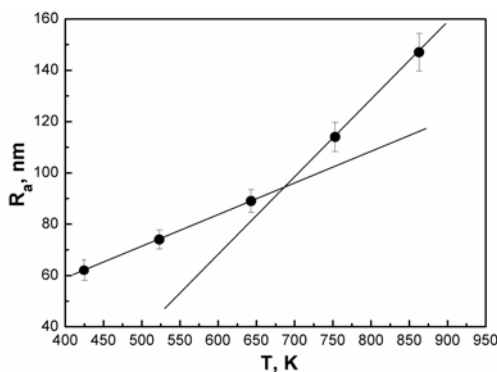
After processing RBS spectra of ZnS, silicon was found near the substrate (we assume that Si atoms diffused from glassceramic to halcogenide under high temperatures of condensation). The small amount of W (~1-2 %) is also on film surface, and it is obviously caused by tungsten evaporator. It is known that the RBS method has a high sensitivity to elements with large atomic number, therefore W is registered despite very small concentration. The oxygen is found only close to the substrate and in the near-surface film layer where oxide phases (ZnO for example) may be formed in the air. It is necessary to mark that in ZnS films obtained by the pyrolitic method and from chemical solutions the oxygen amount dissolved in halcogenide may run up to 3-8 % and such films can be rather considered to be a solid solution $ZnS_x O_{1-x}$ or mixture ZnS, $Zn(OH)_2$ and ZnO [10]. In vacuum condensates, the oxygen amount don't exceed 1-2 % (usually). That is registered experimentally. Although the carbon trace (<1 %) is detected on examined films surface but, as the additional investigation argues, this element penetrates into the sample from vacuum oil.
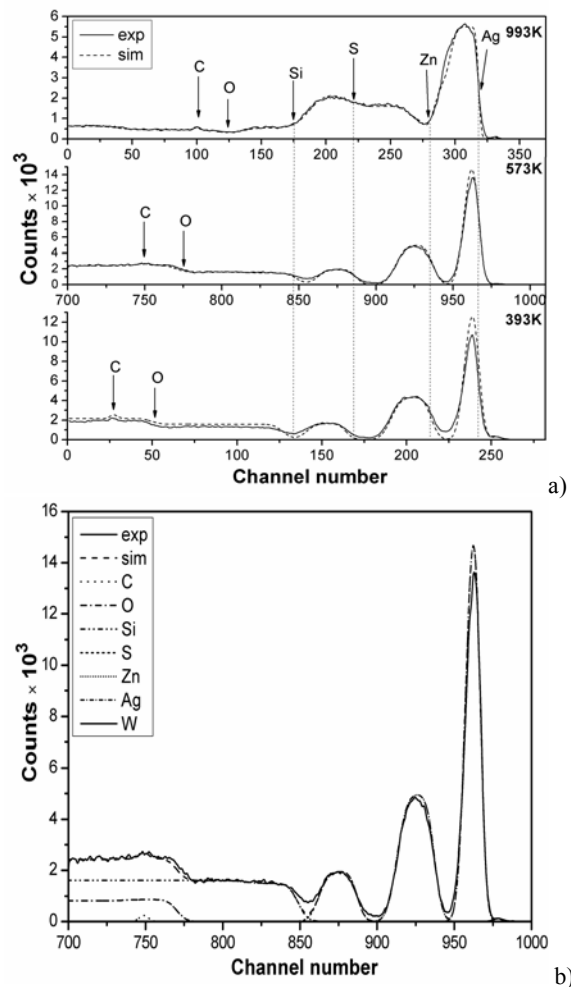

Fig. 4. RBS spectra of 1 MeV protons, scattered from Ag/ZnS/glassceramic (a) and example of simulation pattern at $T_s = 573$ K (b).

Fig. 3. The average arithmetic film profile deviation R_a vs T_s.

RBS spectra analysis enabled to calculate the layer thickness and component concentrations of compound. The ZnS film thickness is determined from the relationship:

$$L = \frac{\Delta E}{[\bar{\varepsilon}]_{ZnS} \cdot n_{ZnS}}, \qquad (1)$$

were ΔE is the energy width of a peak; n_{ZnS} - concentration of ZnS compound; $[\bar{\varepsilon}]_{ZnS}$ − "stopping" cross-section of ZnS calculated from Bragg's rule through "stopping" cross-sections of the different compound elements:

$$[\bar{\varepsilon}]_{ZnS} = [\bar{\varepsilon}]_{Zn} c_1 + [\bar{\varepsilon}]_S c_2, \qquad (2)$$

$$n_{ZnS} = \frac{\rho_{Zn} c_1 + \rho_S c_2}{A_{Zn} c_1 + A_S s_2} N_A, \qquad (3)$$

here ρ_{Zn}, ρ_S are the densities of individual elements, respectively; A_{Zn}, A_S are their atomic masses; c_1 and c_2 − weighting factors.

The film thicknesses average ratio of atomic concentrations of compound components was determined using the formulae

$$\gamma = \frac{C_{Zn}}{C_S} = \frac{\sigma_S H_{Zn} \Delta E_{Zn}}{\sigma_{Zn} H_S \Delta E_S}, \; c_1 = \frac{\gamma}{1+\gamma}, \; c_2 = \frac{\gamma}{1+\gamma}, \quad (4)$$

where C_{Zn}, C_S are atomic percentage of Zn and S, respectively; σ_{Zn}, σ_S − cross-sections of protons scattered by Zn and S; ΔE_{Zn}, ΔE_S − energetic width (FWHM) of a peak for Zn and S, respectively; H_{Zn}, H_S − the magnitudes of a signal for Zn and S, respectively.

For the RBS data, the thicknesses of ZnS films were determined. The spectra of these films are shown in Fig. 4. The thicknesses L are 194±5, 178±5, and 450±5 nm for the samples deposited under temperatures T_s equal to 393, 573, and 993 K, respectively.

The investigations show that for L > 300 nm and proton energies $E_0 = 1$ MeV overlapping of partial peaks takes place that complicates the data processing. In fact, Fig. 4a shows that peaks are separated for L = 178 nm and 194 nm, but for L = 450 nm peaks are overlapped.

RBS method also allows determining the depth profile of layer components. For the case when partial peaks are separated on RBS spectra, the component concentrations of compound, ratio γ and stoichiometry changes with the layer thickness were calculated. With this, it was considered that the condensates are area homogeneous.

In Fig. 5, the Zn-to-S ratios of ZnS compound as a function of depth for temperatures T_s = 393 K and 573 K are represented.
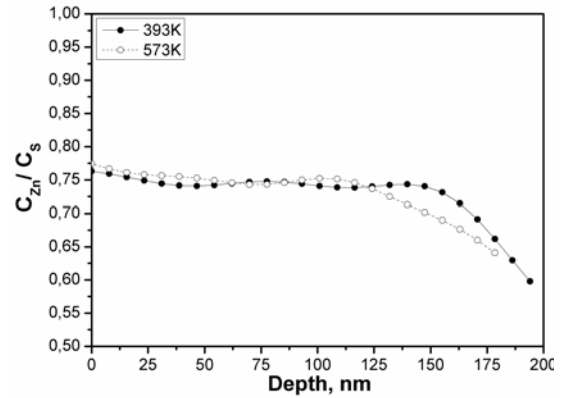

Fig. 5. Dependence of ZnS films stoichiometry on depth for Ag/ZnS/glassceramic structure.

As seen from Fig. 5, layer stoichiometry is lightly varying with depth, and the S concentration is increased in the interlayer that adjoins the substrate. It is the evidence of evaporation incongruence of ZnS compound under deposition process. It appears also that condensate stoichiometry is determined by the substrate temperature T_s and depends on the film thickness. The stoichiometry depending on these parameters was varying from 0.72 to 1.07. The obtained ratios of the component concentrations for ZnS films ($\gamma \sim 0.72$) are somewhat unexpected and require refinement using other methods. The analogous data are published only in the paper [11]. It will be possible in the case of RBS data that ZnS films must be two-phase and contain inclusions of S. But this contradicts results of X-ray diffraction study and scanning electron and optical microscopy. By means of these methods the S precipitates are not detected in films. But it is necessary to point out that our X-ray diffraction and electron microscopy investigations were fulfilled using more thick films ($L \sim 3$-5 µm). The concentration ratios $\gamma = 1.07$ found for these films ($L = 450$ nm) correspond to published data. As a rule, ZnS films obtained by various methods reveal the Zn excess [12-14].

The interdiffusion of elements was observed in the interface between Ag and ZnS that is related with applying the metal contact over heated substrate. While the calculation results of "spreading" magnitudes of Zn and S distribution profiles in this transition layer are quantitatively and qualitatively harmonized with the data of film surface roughness measurements.

4. Conclusions

The surface morphology investigation and nondestructive elemental analysis of many-layer Ag/ZnS/glassceramic structure obtained by close-spaced vacuum sublimation technique under different grow temperatures were carried out. Two temperature ranges where the film growth is realized by different mechanisms were determined. It was established that the layer surface roughness was significantly increased in the region of columned growth.

By means of the RBS method, the elemental composition of condensates was determined, and component distribution of compound as a function of many-layer system depth was obtained. The impurities including oxygen are revealed only near the film surface and in layer contacting with substrate. It was shown that thickness averaged stoichiometry of ZnS films were determined by deposition regimes and were varying in Zn-to-S ratio range 0.72-1.07.

The fulfilled studies indicate the CSVS method availability of deposition of ZnS films, suitable for using as high-bandgap window of solar cells.

Acknowledgement

References

1. K. Ramanathan, M.A. Contreras, C.L. Perkins *et al.*, Properties of 19.2 % efficiency ZnO/CdS/CuInGaSe$_2$ thin-film solar cell // *Progr. Photovolt.: Res. Appl.* **11,** p. 225 (2003).
2. M.A. Contreras, T. Nakada, M. Hongo *et al.* // *Proc. 3rd World Conference of Photovoltaic Energy Conversion*, Osaka, Japan, p. 570 (2003).
3. D. Hariskos, S. Spiering, M. Powalla, Buffer layers in Cu(In,Ga)Se$_2$ solar cells and modules // *Thin Solid Films* **480-481**, p. 99-109 (2005).
4. Y.P.V. Subbaiah, P. Prathap, M. Devika, K.T.R. Reddy, Close-spaced evaporated ZnSe films: preparation and characterization // *Physica B* **365**, p. 240 (2005).
5. *ISO Recommendations on Roughness Measurements*. ISO/R 468, 1878, 1880, TC 57.
6. J.R. Tesma, M. Nastasi, J.C. Barbow *et al*., *Handbook of Modern Ion Beam Materials Analysis*. Materials Research Society, Pittsburgh, 1995.
7. L.C. Feldman, J.W. Mayer, *Fundamentals of Surface and Thin Film Analysis*. North Holland-Elsevier, New York, 1986.
8. D.I. Kurbatov, A.S. Opanasyuk, Optical properties ZnS thin films for the antireflection coating of solar cells // *Visnyk Sumskogo Derzhav. Universitetu* **2**, p. 60-66 (2008) (in Ukrainian).
9. H.H. Andersen, J.F. Ziegler, *Hydrogen Stopping Powers and Ranges in All Elements*. Pergamon Press, New York, 1977.
10. A.O. Pudov, J.R. Sites, T. Nakada, Performance and loss analyses of high-efficiency chemical bath deposition (CBD)-ZnS/Cu(In$_{1-x}$Ga$_x$)Se$_2$ thin-film solar cells // *Jpn J. Appl. Phys.* **41**(Part 2), p. 672-674 (2002).
11. R. Kobayashi, N. Sato, M. Ichimura, E. Arai, Photochemical deposition of ZnS thin films from C$_4$H$_4$KNaO$_6$-added solutions // *J. Opt. and Adv. Mat.* **5**(4), p. 893-898 (2003).
12. H. Kashani, Production and evaluation of ZnS thin films by the MOCVD technique as alpha-particle detectors // *Thin Solid Films* **288**, p. 50-56 (1996).
13. I.O. Oladeji, L. Chow, Synthesis and processing of CdS/ZnS multilayer films for solar cell application // *Thin Solid Films* **474**, p. 77-83 (2005).
14. S.J. Yun, S. Dey, K.S. Nam, Zinc sulfide and terbium doped zinc sulfide films grown by traveling wave reactor atomic layer epitaxy // *J. Korean Phys. Soc.* **33**, p. 454-457 (1998).